

## **An ANC algorithm based on an adjustable phase shifter without secondary path modeling**

**Chen, Kai**<sup>1</sup>

Key Laboratory of Modern Acoustics, Institute of Acoustics, Nanjing University  
Nanjing 210093, China

**Lu, Jing**<sup>2</sup>

Key Laboratory of Modern Acoustics, Institute of Acoustics, Nanjing University  
Nanjing 210093, China

### **ABSTRACT**

**Abstract:** The ANC (active noise control) algorithm always suffers from an auxiliary modelling process with adaptive filtering. One type of perturbation based algorithm applies a phase response on the reference signal in each frequency bin instead of the estimation of the secondary path. However, the values of the potential phases angles are fixed which limits the convergence performance of the ANC system. In this paper, we propose an active noise control's algorithm based on the method in which the phase shifter for the reference signal can be adjusted according to the results of the signal monitoring. Compared with the other algorithms of this type, the proposed algorithm has a superiority in convergence performance, which is proved by simulation results.

**Keywords:** Active noise control

**I-INCE Classification of Subject Number:** 38

### **1. INTRODUCTION**

Active noise control (ANC) is an efficient means to reduce noise based on the superposition principle. In the ANC system, the undesired noise in certain area can be cancelled by the artificial sound with a similar amplitude but opposite phase, which is brought forth by some secondary sources, such as loudspeakers and actuators. The ANC has received much attention from a wide range of academic and industrial applications for its higher flexibility and better performance on low frequency noise reduction [1, 2]. The filter-x least mean square (FxLMS) algorithm is the most common algorithm used in the ANC system due to its ease of implementation. However, it is inconvenient for the most active noise control systems available for practical applications because of the requirement for an off-line identification of the secondary path from the control source to the error microphone [3], especially in the situation that the secondary path is time-varying.

---

<sup>1</sup> chenkai@nju.edu.cn

<sup>2</sup> lujing@nju.edu.cn

In order to settle this issue, many techniques and methods have been proposed. The online identification with additional noise is widely used in practical applications, in which an auxiliary random noise is added to model the secondary path online by adaptive filtering [4-6]. However, the overall noise reduction of the ANC system will be affected since the additive noise increases the residual noise level.

The algorithms based on the overall modelling methods have been also developed, in which the output of the secondary source is used to model the secondary path directly [7-10]. The main disadvantage is its considerable computational burden because at least three transfer functions need to be matched simultaneously at every sampling interval even when the secondary is unchanged. Otherwise, the secondary-path estimated obtained by the overall modelling technique depends on the frequency content of the primary noise, which may not have sufficient excitation over the entire band and furthermore may be changing. And it may lead to instability of the ANC system.

In recent years, another new type of algorithms has been proposed. These algorithms are based on the thought that a phase shifter is applied on the reference signal in frequency bins rather than the real secondary path for adaptive processing [11-14], which is named phase shifter based algorithm herein. The angle of the phase shifter is always chosen from several some potential phase angles to achieve the best convergence performance. The type of algorithm is usually implemented in the frequency domain or in subband architecture. These algorithms are attractive due to their simple implementation and good performance. We will concentrate on the improvement of this type of algorithm in the paper. However, the potential phase angles in these algorithms are set as two or four unchanged options in advance, and the true phase direction may often be still far from the final selected phase, which can cause a long convergence period and even influence the ANC system's stability. In order to overcome it, an algorithm based on an adjustable phase response will be proposed in this paper. The phase shifter for the reference signal can be re-calculated based on the results of the signal monitoring during the system's convergence.

We arrange this paper as follows. In Section 2, the ANC algorithm method which applies the angle shifter on the reference signal is discussed briefly. Then, a new ANC algorithm with an adjustable phase response is introduced in Section 3. The simulation results of our proposed ANC algorithms are given in Section 4. We conclude our discussion in Section 5.

## 2. THE PHASE SHIFTER BASED ANC ALGORITHM

The FxLMS algorithm structure is illustrated in Figure 1(a). In the Figure 1(a),  $x(n)$  is the reference signal,  $P(z)$  is the primary path transfer function,  $W(z)$  is the adaptive control filter,  $y(n)$  is the output of the secondary source,  $e(n)$  is the actual control signal at the position of the error sensor;  $C(z)$  is the true secondary path and  $\hat{C}(z)$  is its estimation;  $z(n)$  is the filtered reference signal. The length of  $W(z)$  is  $N^W$  and its  $i$ -th tap coefficient at the time index  $n$  is  $w_i(n)$ . The length of  $\hat{C}(z)$  is  $N^{\hat{C}}$  and its  $i$ -th tap coefficient at the time index  $n$  is  $\hat{c}_i(n)$ . The FxLMS algorithm can be summarized as

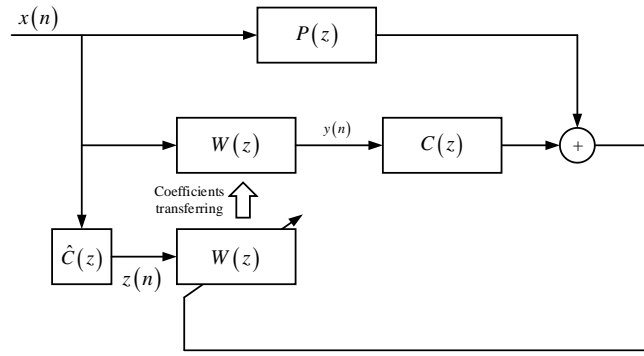
$$\begin{cases} y(n) = \sum_{i=0}^{N^W-1} w_i(n)x(n-i) \\ z(n) = \sum_{i=0}^{N^{\hat{C}}-1} \hat{c}_i(n)x(n-i) \\ w_i(n+1) = w_i(n) - \mu \cdot z(n-i) \cdot e(n), \end{cases} \quad (1)$$

where  $\mu$  is the step-size. The residual noise error at the error sensor is

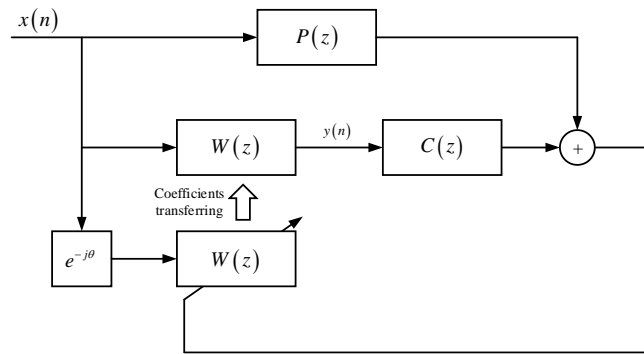
$$e(n) = \sum_{i=0}^{N^p-1} p_i x(n-i) + \sum_{i=0}^{N^c-1} c_i y(n-i), \quad (2)$$

where the lengths of  $P(z)$  and  $C(z)$  are  $N^p$  and  $N^c$ , and the  $i$ -th coefficients of  $P(z)$  and  $C(z)$  are  $p_i$  and  $c_i$ , respectively.

Compared with the FxLMS algorithm, the phase shifter based algorithm applied a phase shifter on the reference signal in the frequency domain, instead of filtering the reference signal by the estimated secondary path, which is shown in Figure 1(b). It is recommended to implement the phase shifter based algorithm in subband architecture due to the low level of interference between each subband. Furthermore, the independent feature of the subband architecture also makes the parallel process possible. Thus, the subband algorithm implementation is focused on in the rest part of this paper. The phase shifter based algorithm proposed in [12] is an attempts in subband implementation, named Wu's algorithm herein. There are four optional potential phase angles to be chosen from for each subband, i.e.,  $0^\circ$ ,  $90^\circ$ ,  $180^\circ$  and  $270^\circ$ . If the true angle of the secondary path is located right between two close items of these angles, such as  $44^\circ$  or  $136^\circ$ , the difference between the approximate angle and the true angle is so large that it can deteriorate the convergence performance and even reduce the system stability. To overcome this problem, we will make an improvement on this type of algorithm which can adjust the phase angles to match the ones of the secondary path in the following part of this paper.



(a)



(b)

Figure 1 The block diagram of the FxLMS algorithm (a) and the phase shifter based algorithm(b).

### 3. THE PROPOSED PHASE SHIFTER BASED ANC ALGORITHM

The phase shifter based ANC algorithm in each subband is similar and independent. The subband index  $[\cdot]_m$  in the following expression is omitted for clarity. The frequency-domain form of the algorithm in each subband can be summarized as

$$\begin{cases} Y(l) = W(l) \cdot X(l) \\ W(l+1) = W(l) - \mu \cdot e^{-j\theta} \cdot X^*(l) \cdot E(l) \\ E(l) = P \cdot X(l) + C \cdot Y(l), \end{cases} \quad (3)$$

where  $l$  is the frame index,  $X(l)$ ,  $Y(l)$  are the frequency expressions of  $x(n)$ ,  $y(n)$  respectively,  $W(l)$  is the frequency expression of control filter at frame  $l$ ,  $P$  and  $C$  are the frequency expressions of the primary path and the estimated secondary path respectively, the superscript  $*$  is the complex conjugate operation.

The strategy of accumulating updating is used in the algorithm, which means that the control filter is updated once every  $\Delta$  decimated samples and is often used in the delayless subband architecture for computation complexity reduction as [15-17]. In details, the control filter at time index  $l+1, l+2, \dots, l+\Delta$  is unchanged as  $W(l)$  until time index  $l+\Delta$ . At time index  $l+\Delta$ , the control filter  $W(l+\Delta)$  is updated as

$$W(l+\Delta) = W(l) + \exp(-j\theta) \cdot \beta(l), \quad (4)$$

where

$$\begin{cases} \beta(l) = Q(l) \cdot [W^\circ(l) - W(l)] \\ Q(l) = \mu \cdot C \cdot \sum_{i=l}^{l+\Delta-1} |X(i)|^2 \\ W^\circ = -P/C. \end{cases} \quad (5)$$

The purpose of the algorithm is to obtain the value of  $\theta$  when the power of  $E(l+\Delta)$  gets the minimum. Because  $W(l+\Delta)$  is concerning to  $\theta$ , so  $W(l+\Delta)$  is rewritten as  $W(l+\Delta, \theta)$ . It is easy to conclude from Eq.(3) that  $E(l+\Delta)$  depends on  $W(l+\Delta, \theta)$  completely, when the reference signal  $X(l)$  is steady enough. Thus,  $E(l+\Delta)$  is also rewritten as  $E(l+\Delta, \theta)$ , that is

$$E(l+\Delta, \theta) = P \cdot X(l+\Delta) + C \cdot Y(l+\Delta). \quad (6)$$

Take Eq.(4) into Eq.(6) to obtain

$$\begin{aligned} & E(l+\Delta, \theta) \\ &= P \cdot X(l+\Delta) + C \cdot [W(l) + \exp(-j\theta) \cdot \beta(l)] \cdot X(l+\Delta) \\ &= X(l+\Delta) \cdot C \cdot [W^\circ(l) - W(l)] \left\{ \exp(-j\theta) \cdot \mu \cdot C \cdot \sum_{i=l}^{l+\Delta-1} |X(i)|^2 - 1 \right\}. \end{aligned} \quad (7)$$

Then, the mean power of  $E(l+\Delta, \theta)$  over the power of the reference signal  $X(l+\Delta)$  is define as

$$R_\theta = \text{Mean} \left\{ \frac{|E(l+\Delta, \theta)|^2}{|X(l+\Delta)|^2} \right\}, \quad (8)$$

which is expressed as

$$R_\theta = U - V \cdot \cos(\varphi - \theta), \quad (9)$$

where,

$$\begin{cases} U = A \cdot (1 + B^2) \\ V = 2 \cdot A \cdot B \\ A = |C \cdot [W^\circ - W(l)]|^2 \\ B = \mu \cdot \sum_{i=l}^{l+\Delta-1} |X(i)|^2 \cdot |C| \\ \varphi = \angle C, \end{cases} \quad (10)$$

where,  $\angle[\cdot]$  denotes complex phase.

The value of  $R_\theta$  in Eq.(9) varies periodically with  $\theta$ . The step-size  $\mu$  is a factor of  $V$ , so we can set  $\mu$  small enough to satisfy  $V < 1$ . Then if  $\theta$  is equal to  $\varphi$ ,  $R_\theta$  reaches the minimum value. In order to get the solution of  $\varphi$  in the Eq.(9), it is easy to create simultaneous equations with at least 3 values of  $\theta$  and their corresponding  $E(l+\Delta, \theta)$  and  $X(l+\Delta)$  by measurement. Therefore, we set  $\theta$  to  $0, \frac{\pi}{2}, \pi, \frac{3\pi}{2}$  respectively, which is based on the following consideration: Eq.(9) is based on the assumption that the all transfer functions are in a steady-state. In opposite word, the solution of  $\varphi$  Eq.(9) is invalid if any transfer function changes during collecting measurement data. With 4 value of  $\theta$ , we can solve the least-square solution of Eq.(9) and then evaluate the validity of the solution by the least-square residual error.

The simultaneous equations by setting  $\theta$  to  $0, \pi/2, \pi, 3\pi/2$  can be expressed as

$$\begin{cases} R_0 = U - V \cos(\varphi) \\ R_{\pi/2} = U - V \cos(\varphi - \pi/2) \\ R_\pi = U - V \cos(\varphi - \pi) \\ R_{3\pi/2} = U - V \cos(\varphi - 3\pi/2), \end{cases} \quad (11)$$

And it can be simplified further as

$$\begin{cases} R_0 = U - V \cos(\varphi) \\ R_{\pi/2} = U - V \sin(\varphi) \\ R_\pi = U + V \cos(\varphi) \\ R_{3\pi/2} = U + V \sin(\varphi). \end{cases} \quad (12)$$

Next, we try to get the least squares solution [18] on Eq.(12) as

$$\begin{cases} \frac{\partial S}{\partial \varphi} = 0 \\ \frac{\partial S}{\partial U} = 0 \\ \frac{\partial S}{\partial V} = 0, \end{cases} \quad (13)$$

where,

$$\begin{aligned} S = & [U - V \cos(\varphi) - R_0]^2 + [U - V \sin(\varphi) - R_{\pi/2}]^2 \\ & + [U + V \cos(\varphi) - R_\pi]^2 + [U + V \sin(\varphi) - R_{3\pi/2}]^2. \end{aligned} \quad (14)$$

Then we have

$$\begin{cases} -R_0 \sin(\varphi) + R_{\pi/2} \cos(\varphi) + R_\pi \sin(\varphi) - R_{3\pi/2} \cos(\varphi) = 0 \\ 4U - R_0 - R_{\pi/2} - R_\pi - R_{3\pi/2} = 0 \\ 2V + R_0 \cos(\varphi) + R_{\pi/2} \sin(\varphi) - R_\pi \cos(\varphi) - R_{3\pi/2} \sin(\varphi) = 0. \end{cases} \quad (15)$$

Because of  $U \geq 0$  and  $V \geq 0$  defined in Eq.(10) and the range of  $\varphi$  is  $[0, 2\pi)$ ,  $\varphi$  can be obtained as

$$\varphi = \begin{cases} \arctan \left[ \frac{R_{3\pi/2} - R_{\pi/2}}{R_\pi - R_0} \right], R_0 \leq R_\pi \\ \pi + \arctan \left[ \frac{R_{3\pi/2} - R_{\pi/2}}{R_\pi - R_0} \right], R_0 > R_\pi. \end{cases} \quad (16)$$

Furthermore, the  $U$  and  $V$  in Eq.(15) can be solved as

$$\begin{cases} U = \frac{R_0 + R_{\pi/2} + R_\pi + R_{3\pi/2}}{4} \\ V = \frac{\sqrt{(R_0 - R_\pi)^2 + (R_{\pi/2} - R_{3\pi/2})^2}}{2}. \end{cases} \quad (17)$$

Then we take  $U$ ,  $V$  and  $\varphi$  back to Eq.(12), and get the  $\hat{R}_0, \hat{R}_{\pi/2}, \hat{R}_\pi, \hat{R}_{3\pi/2}$ , which are the estimates of  $R_0, R_{\pi/2}, R_\pi, R_{3\pi/2}$  respectively. Define the regularized sum residual error of the least-square approximation  $\rho$  as

$$\rho = \frac{\sqrt{(\hat{R}_0 - R_0)^2 + (\hat{R}_{\pi/2} - R_{\pi/2})^2 + (\hat{R}_\pi - R_\pi)^2 + (\hat{R}_{3\pi/2} - R_{3\pi/2})^2}}{R_0 + R_{\pi/2} + R_\pi + R_{3\pi/2}}. \quad (18)$$

We can use  $\rho$  to assess the validity of  $\varphi$  calculated by Eq.(16). The smaller the value of  $\rho$  is, the more correct  $\varphi$  is.

Based on the above discussion, the proposed algorithm is detailed in Table 1.

Compared with the traditional phase shifter based ANC algorithm, the proposed algorithm just introduces some operations Eq.(16), Eq.(17) and (18) in each subband after acquiring the measure residual error. So the increased computational complexity in the proposed algorithm is tolerant completely.

Before submitting the manuscript you will be required to pay at least one registration. Additionally, if you are submitting more than one manuscript, there is an additional nominal charge for each additional manuscript submitted.

Table 1 The subband ANC algorithm based on an adjustable phase direction without secondary path estimation.

Stage	Step No.	Description*
A	1	Initialize the adaptive controller coefficients $w_{i,m}(0)$ and the step-size $\mu_m$ .
B	2	Set $\theta = 0$ and run adaptive filtering as Eq.(5) for $\Delta$ frames to get the adaptive increase term $\beta(l)$ .
C	3	Obtain the potential control filter of $W_m^{\theta_m^i}(k + \Delta)$ for each $\theta_m^i(k)$ with Eq.(4). Apply the filter on the reference signal in turn for $P$ frames and measure the residual noise error power $R_\theta$ .
	4	Update the main phase direction $\varphi$ by Eq.(16).
	5	Calculate the $\rho$ to evaluate the validity of $\varphi$ .
	6	If $\rho > \rho_T$ , which means that the value of $\varphi$ is valid, repeat 2-5 until the phase direction value $\varphi$ is correct.
D	7	Update the control filter with the main phase estimated in Stage C. If some exception happens, such as divergence, go to step 2.

Note: \* All the processes are performed in each subband in parallel.

#### 4. SIMULATION RESULTS

In this simulation, the proposed algorithm was compared with Wu's algorithm [12]. The sampling rate is 2400 Hz. The subband number is 128 and the decimation Factor is 64. The length of the proto-type filter for subband analysis and synthesis is 1024. The control filter length in fullband is 512. The reference signal is Gauss white noise. The  $\Delta$  for the accumulating updating process is set to be 100. The frame number to measure  $R_\theta$  is set to be 100. The coefficients of the control filter in subband are initialized to 0. The step-size in each subband is set to be the largest possible value to assure that the adaptive filter converges at the fastest speed while remaining stable. The primary path and secondary path used in the simulation are both shown in Figure 2.

Figure 3 gives the results of the phase angle approaching in each subband. It is obvious that the calculated phase angle in the proposed algorithm is much closer to the one of the practical secondary path. Figure 4 gives the  $\rho$  value in each subband. The values of  $\rho$  are small enough, which prove the validity of the calculated phase.

The convergence performance of the system is shown in Figure 5. During the first 13.3 s, the two algorithms are both approaching the most approximate phase for consequent adaptive processing. The proposed algorithm has a faster convergence speed and lower residual error within the observation time scale, due to its better results of the

phase direction's matching. Figure 6 demonstrates the tracks of the complex value of the control filter in two subbands. It is obvious that the proposed algorithm approaches to the optimal value more directly than the Wu's algorithm, which guarantees the convergence performance and the system's stability.

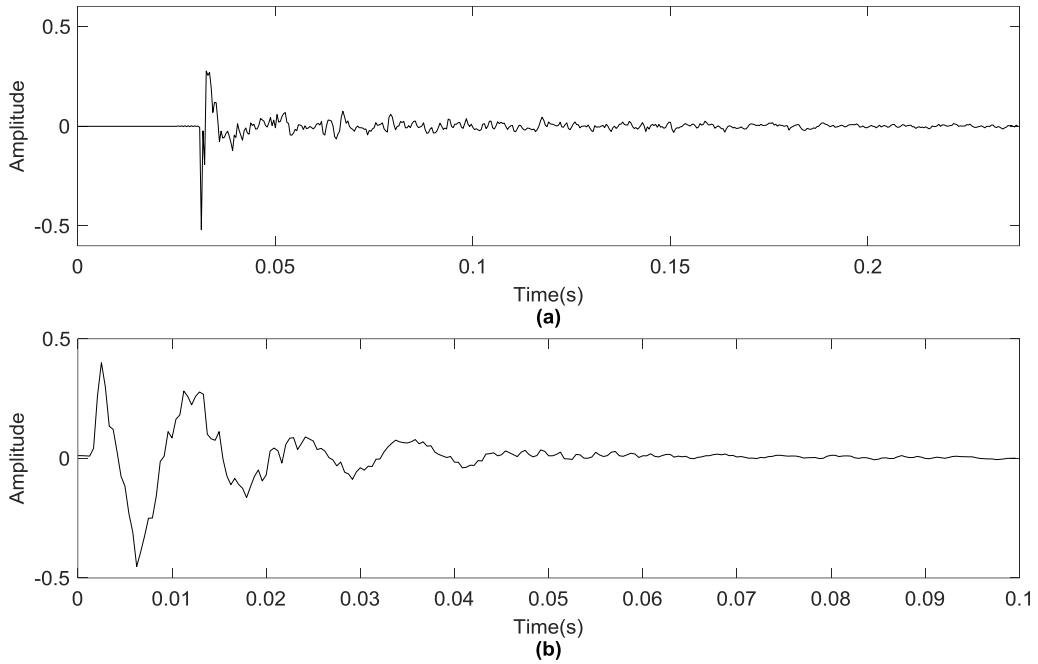


Figure 2 The time-domain impulse response of the primary path (a) and the secondary path (b) for the simulation.

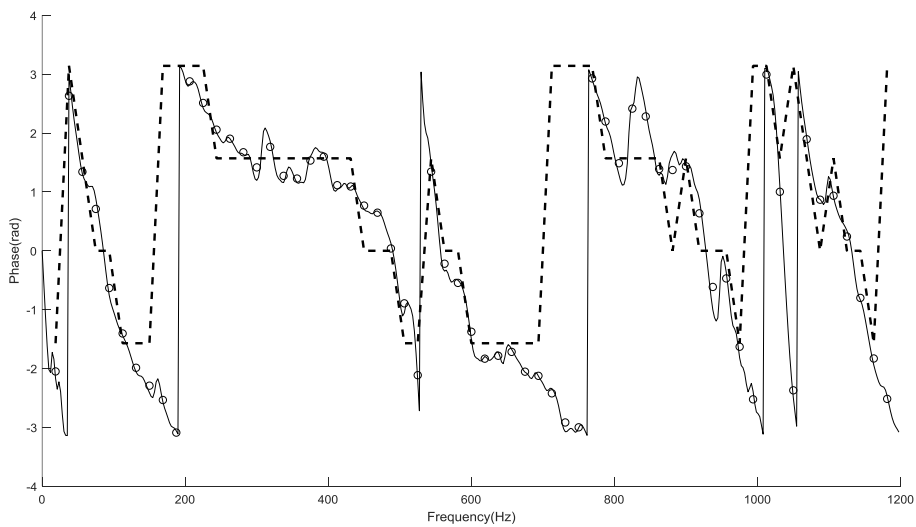


Figure 3 Comparison of the estimated phases with the real phase of the secondary path. The



real phase (solid line), the proposed algorithm (circle) and Wu's algorithm (dashed line).

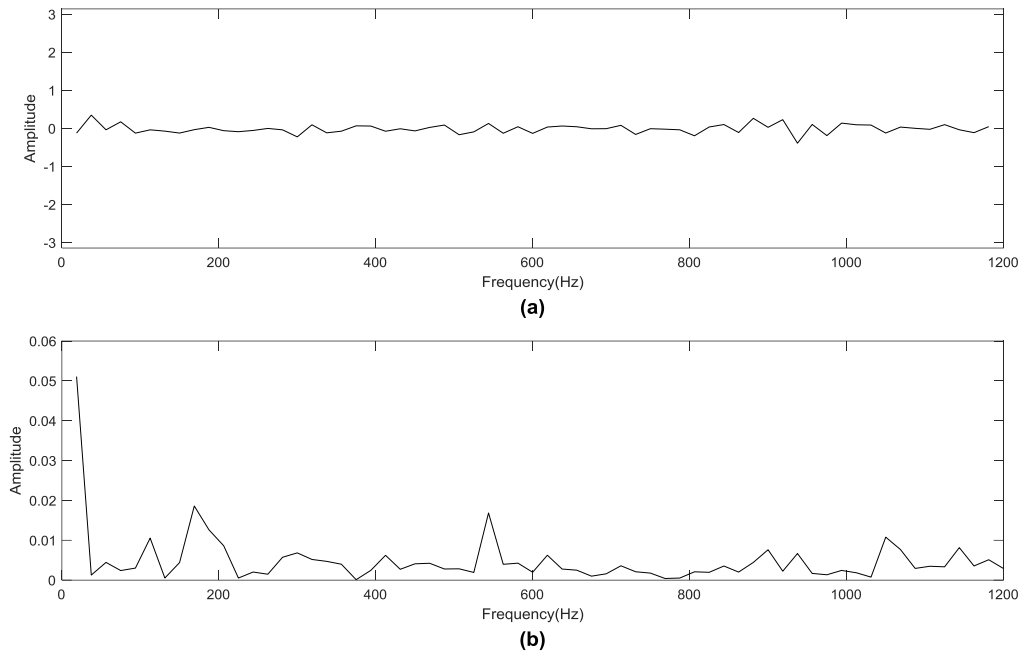


Figure 4 The difference of the phase (a) and the  $\rho$  which used to check the validity of the estimated  $\varphi$  in the frequency domain (b).

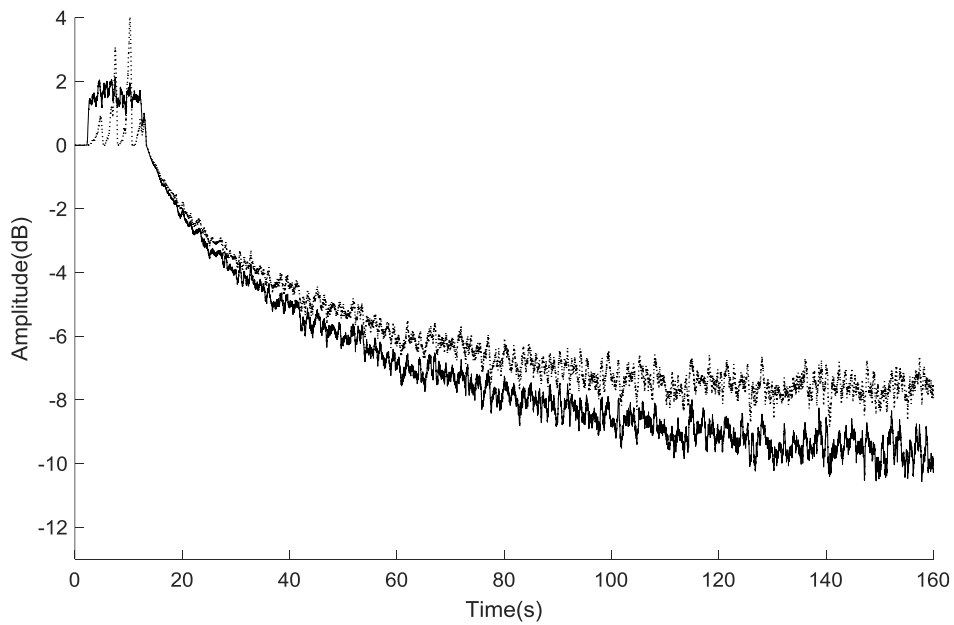
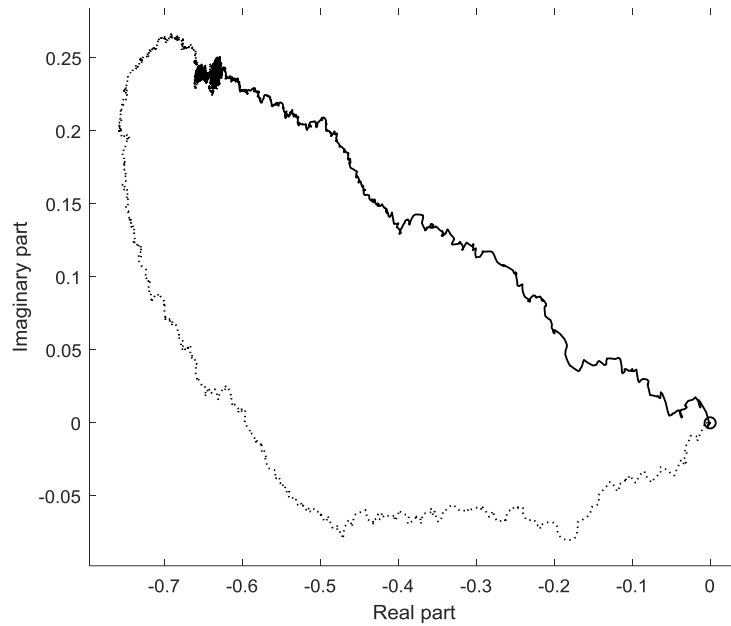
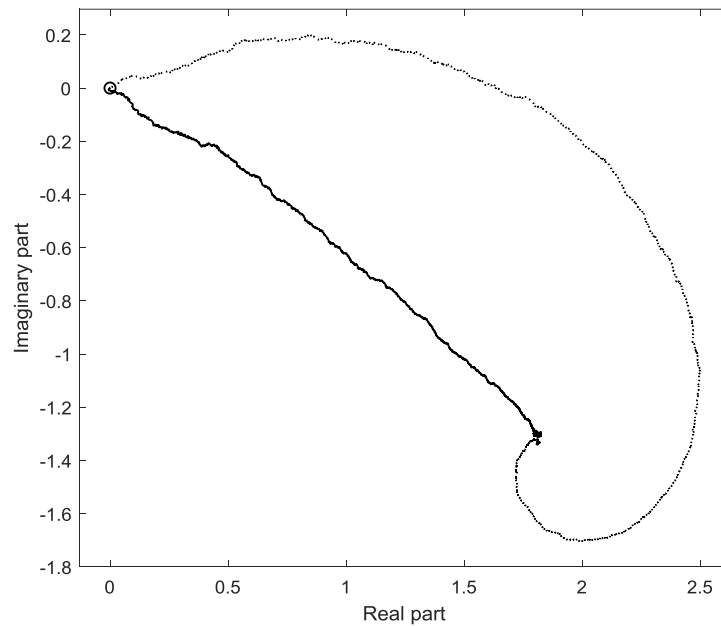


Figure 5 Convergence curve comparison. The proposed algorithm (solid line) and Wu's algorithm (dotted line). Before 13.3 s, the two algorithms are both searching the optimal phase for consequent adaptive processing.



(a)



(b)

Figure 6 The convergence tracks in the 9-th subband (a) and the 24-th subband(b). The proposed algorithm (solid line) and Wu's algorithm (dotted line).

## 5. CONCLUSIONS

In this paper, we proposed an active noise control's algorithm based on the phase shifter method in which the phase shifter for the reference signal can be adjustable according to the results of the signal monitoring. Compared with the traditional phase shifter based algorithms, the proposed algorithm has better performance in the system convergence, which is also demonstrated by simulation results.

## 6. ACKNOWLEDGEMENTS

This work was supported by the National Natural Science Foundation of China (Grant Nos. 11874219 and 11874218) and the Fundamental Research Funds for the Central Universities.

## 7. REFERENCES

1. Elliott, S.J. and P.A. Nelson, *Active noise control*. IEEE signal processing magazine, 1993. **10**(4): p. 12-35.
2. Kuo, S.M. and D.R. Morgan, *Active noise control: a tutorial review*. Proceedings of the IEEE, 1999. **87**(6): p. 943-973.
3. Kuo, S.M. and D. Morgan, *Active noise control systems: algorithms and DSP implementations*. 1995: John Wiley & Sons, Inc.
4. Eriksson, L.J. and M.C. Allie, *Use of random noise for on -line transducer modeling in an adaptive active attenuation system*. The Journal of the Acoustical Society of America, 1989. **85**(2): p. 797-802.
5. Akhtar, M.T., M. Abe, and M.J.I.T.o.S. Kawamata, *A new structure for feedforward active noise control systems with improved online secondary path modeling*. IEEE Transactions on Speech Audio Processing, 2005. **13**(5): p. 1082-1088.
6. Xiao, Y., L. Ma, and K.J.I.T.o.S.P. Hasegawa, *Properties of FXLMS-based narrowband active noise control with online secondary-path modeling*. 2009. **57**(8): p. 2931-2949.
7. Fujii, K., M. Muneyasu, and J. Ohga, *Active noise control system using the simultaneous equation method without the estimation of error path filter coefficients*. Electronics & Communications in Japan, 2002. **85**(12): p. 101-108.
8. Sano, A. and Y. Ohta. *Adaptive active noise control without secondary path identification*. in *IEEE International Conference on Acoustics, Speech, and Signal Processing, 2003. Proceedings*. 2003.
9. Jin, G.Y., et al., *A simultaneous equation method-based online secondary path modeling algorithm for active noise control*. Journal of Sound & Vibration, 2007. **303**(3-5): p. 455-474.
10. Chen, K. and J. Lu. *Kalman filter based active noise control algorithm with simultaneous transfer function modeling*. in *INTER-NOISE and NOISE-CON Congress and Conference Proceedings*. 2018. Institute of Noise Control Engineering.
11. Zhou, D. and V. DeBrunner, *A new active noise control algorithm that requires no secondary path identification based on the SPR property*. IEEE Transactions on Signal Processing, 2007. **55**(5): p. 1719-1729.
12. Wu, M., G. Chen, and X. Qiu, *An improved active noise control algorithm without secondary path identification based on the frequency-domain subband architecture*. IEEE Transactions on Audio Speech and Language Processing, 2008. **16**(8): p. 1409-1419.
13. Gao, M., J. Lu, and X. Qiu, *A simplified subband ANC algorithm without secondary path modeling*. IEEE/ACM Transactions on Audio, Speech, and Language Processing, 2016. **24**(7): p. 1164-1174.
14. Das, K.M., et al., *All-pass filtered x least mean square algorithm for narrowband active noise control*. 2018. **142**: p. 1-10.
15. Morgan, D.R. and J.C. Thi, *A delayless subband adaptive filter architecture*. IEEE Transactions on Signal Processing, 1995. **43**(8): p. 1819-1830.
16. Merched, R., P.S.R. Diniz, and M.R. Petraglia, *A new delayless subband adaptive filter structure*. IEEE Transactions on Signal Processing, 1999. **47**(6): p. 1580-1591.
17. Milani, A.A., et al., *A new delayless subband adaptive filtering algorithm for active noise control systems*. 2009. **17**(5): p. 1038-1045.
18. Kreyszig, E., *Advanced engineering mathematics*. 2010: John Wiley & Sons.